

SPECTRAL REFLECTANCE OF POLY-
CRYSTALLINE STANNIC OXIDE

By

LEE ROY MATTHIESEN

"
Bachelor of Science
Oklahoma State University
Stillwater, Oklahoma
1960

Master of Science
Kansas State Teachers College
Emporia, Kansas
1964

Submitted to the Faculty of the Graduate College
of the Oklahoma State University
in partial fulfillment of the requirements
for the Degree of
DOCTOR OF EDUCATION
July, 1972

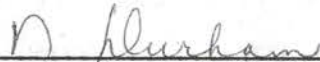
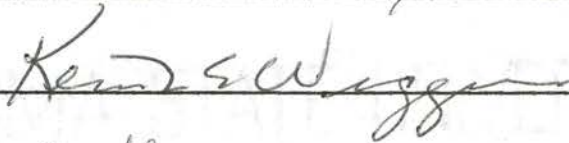
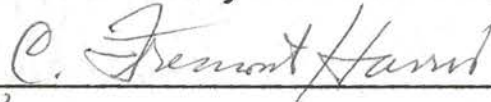
AUG 16 1973

SPECTRAL REFLECTANCE OF POLY-
CRYSTALLINE STANNIC OXIDE

Thesis Approved:



Thesis Adviser



Dean of the Graduate College

ACKNOWLEDGEMENTS

I wish to express my appreciation to my adviser, Dr. E. E. Kohnke, who suggested this most interesting study, provided valuable guidance, and secured financial aid when it was needed. I will always be indebted to Dr. Lee Rutledge and Dr. L. W. Schroeder who turned me on to physics many years ago through their enthusiastic commitment to the beginning physics courses.

Many thanks to my typist, Mrs. Janet Sallee, who did much of the leg work necessary to the completion of this thesis.

Finally, to my wife and family for their patience, encouragement, and assistance during the completion of this work, a most sincere thanks.

TABLE OF CONTENTS

Chapter	Page
I. INTRODUCTION.	1
II. THEORY.	4
III. INSTRUMENTATION AND EXPERIMENTAL DETAILS.	16
IV. EXPERIMENTAL RESULTS.	26
V. CONCLUSIONS	34
SELECTED BIBLIOGRAPHY	44

LIST OF TABLES

Table	Page
I. A Comparison of kd Values From Johnson, Melamed, and Simons Models.	13
II. Sample Preparation Treatments.	24

LIST OF FIGURES

Figure	Page
1. K-M Representation of a Layer of Absorbing and Light-Scattering Particles	4
2. Johnson's Parallel Layer Model	9
3. A Comparison of K-M Remission Function With the Absorption Coefficient From Simmons Model	15
4. Integrating Sphere Attachment for a D-K 1 Spectrophotometer.	19
5. Effect of Firing Temperature on the Relative Reflectance .	27
6. Effect of Firing Time at 1240°C on the Relative Reflectance.	28
7. Effect of Firing Time at 1400°C on the Relative Reflectance.	29
8. Effect of Doping With 0.7% ZnO on the Relative Reflectance	30
9. Degradation of Relative Reflectance With U-V Light	31
10. Temperature Shift of the Absorption Edge	33
11. Relative Reflectance Versus Photon Energy.	38
12. Extrapolation to Find an Allowed Band Transition	41

CHAPTER I

INTRODUCTION.

Considerable study has been done on stannic oxide (SnO_2) in recent years. Finding appropriate samples is difficult, as pure, laboratory grown, crystals are relatively hard to come by. Corning Glass Works (1) has been able to grow single crystals from the vapor phase with volumes as large as 0.3 cubic centimeters. Obtaining optical parameters by the methods of transmission spectra analysis and specular reflectance (that part of the reflection that obeys the law of reflection and is governed by the well-known Fresnel equation) analysis requires the use of such large smooth single crystals. At Oklahoma State University, several studies have been made using polycrystalline SnO_2 ceramics which are relatively easy to produce in any size and shape. A large part of the reflection from these ceramics is diffuse reflection in which the light leaves the surface traveling in all directions. In this type of reflection, the light penetrates into the interior of the sample and its re-emission depends to a large extent on the particulate nature of the material. The light reflected from a "perfectly diffusing" material obeys the Lambert cosine law which requires that the reflected radiation be distributed symmetrically with respect to the surface normal without regard to the angle of incidence. This study involves development of instrumentation for measurement of diffuse reflectance spectra from such ceramics and the means of obtaining optical properties from such infor-

mation. These optical properties will then be compared with those obtained by other methods.

Houston and Kohnke (2) have proposed an energy level scheme for grown SnO_2 single crystals showing a band gap of approximately 4.0 eV and other levels at 0.21 eV, 0.52 eV, 0.6 eV, 1.0 eV, 1.3 eV, and 1.8 eV below the conduction band. They also indicate that an unresolved level exists between 2.0 eV and the valence band.

Summitt, Marley, and Borelli (3) studied the UV absorption edge in single crystals using polarized light with the electric field parallel to the optical axis ($E \parallel C$) and with the electric field perpendicular to the optical axis ($E \perp C$). They report for $E \parallel C$ a direct gap of 3.93 eV and an indirect gap of 3.7 eV. For $E \perp C$ they found a direct gap of 3.57 eV and an indirect gap of 3.4 eV. They account for these differences by adopting two distinct band gaps 0.3 eV apart.

Nagasawa and Shionoya (4) achieve the almost identical results of 3.89 eV and 3.7 eV for $E \parallel C$ and 3.57 eV and 3.4 eV for $E \perp C$. From their published graphs one can calculate a temperature shift of -1.2×10^{-3} eV/ $^{\circ}\text{K}$ for both polarizations in a temperature range of 295°K to 370°K .

Lyashenko and Miloslavskii (5) studying SnO_2 thin films, report a temperature shift of -6×10^{-4} eV/ $^{\circ}\text{K}$ for the fundamental absorption edge and an absorption coefficient of around $3 \times 10^3 \text{ cm}^{-1}$ at 0.35 microns. Kohnke (6) also reports a temperature shift of -6×10^{-4} eV/ $^{\circ}\text{K}$ on natural single crystals.

Ishiguro, Sasaki, Ari and Imai (7) report an absorption coefficient of around $9 \times 10^3 \text{ cm}^{-1}$ for thin SnO_2 films.

Several members of the Solid State and Surface Studies Research Group at Oklahoma State University have reported effects, other than

optical effects, that are related to the chemisorption of oxygen on SnO_2 surfaces. This study will also involve a search for an optical characteristic that can be identified with chemisorption of oxygen, as particulate materials like SnO_2 ceramics have a large effective surface area for such chemisorption processes and thus should be ideal for revealing an optical counterpart.

CHAPTER II

THEORY

Of the many theories used to interpret diffuse reflectance spectra from particulate materials, in terms of conventional optical parameters, the model of Kubelka and Munk (K-M) (8) appears to be the most widely used. Many authors (9, 10, 11, 12) give English discussions of this work. The nomenclature and treatment given here follow reference 9.

Consider a layer of thickness dx a distance x below the surface of a material composed of absorbing and light-scattering particles whose dimensions are much smaller than dx . This surface is illuminated with perfectly diffuse radiant flux whose normal component into the surface is I_0 . The normal component of the flux leaving the surface is J_0 . Considering the material to be an ideal diffuser (i.e., the intensity is the same in all directions) one can show that the average path length for the flux through the infinitesimal layer is $2dx$.

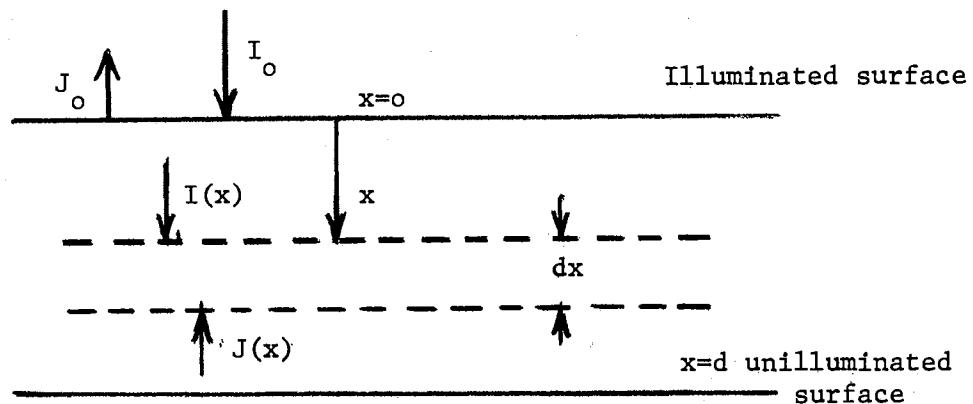


Figure 1. K-M Representation of a Layer of Absorbing and Light-Scattering Particles

Let ϵ be the fraction of light absorbed per unit path length and σ be the fraction of light scattered per unit path length in the sample. If one considers the reduction in downward flux due to absorption and scattering from the initially downward radiation and then increases this by the downward scattering of an initially directed upward flux, one can write an equation for the differential change in the downward intensity due to its passage through the layer dx , namely:

$$dI = -(\epsilon + \sigma) I \cdot 2dx + \sigma J \cdot 2dx$$

Likewise for the upward intensity through the layer

$$dJ = (\epsilon + \sigma) J \cdot 2dx - \sigma I \cdot 2dx$$

letting $K = 2\epsilon$ and $s = 2\sigma$ we find the solutions to these differential equations have the form

$$I = A(1 - \beta) e^{\alpha x} + B(1 + \beta) e^{-\alpha x}$$

and

$$J = A(1 + \beta) e^{\alpha x} + B(1 - \beta) e^{-\alpha x}$$

where

$$\alpha \equiv [K(K + 2s)]^{1/2}$$

and

$$\beta \equiv \frac{\alpha}{K + 2s} = [K/(K + 2s)]^{1/2}$$

with A and B to be determined by the boundary conditions

$$I = I_0 \text{ for } x = 0$$

and

$$I = I_{x=d}, \quad J = 0 \text{ for } x = d$$

The transmittance, T , of the layer is

$$T \equiv \frac{I_{x=d}}{I_0} = \frac{4\beta}{(1 + \beta)^2 e^{\alpha d} - (1 - \beta)^2 e^{-\alpha d}}$$

upon substitution of the constants A and B . It can be seen from this that in the limit of no scattering

$$\sigma = 0$$

$$\text{so } s = 0$$

$$\text{and } \alpha = K, \quad \beta = 1$$

we have

$$T = e^{-Kd}$$

which is the Beer-Lambert law with K playing the role of the conventional absorption coefficient k .

In a similar manner the diffuse reflectance is defined and expressed as

$$R \equiv \frac{J_{x=0}}{I_0} = \frac{(1 - \beta^2)(e^{\alpha d} - e^{-\alpha d})}{(1 + \beta)^2 e^{\alpha d} - (1 - \beta)^2 e^{-\alpha d}}$$

When d is increased until no additional increase in R occurs (a few millimeters for powdered samples) then, setting $d = \infty$, we have

$$R_{\infty} = \frac{1 - [K/(K + 2s)]^{1/2}}{1 + [K/(K + 2s)]^{1/2}}$$

where R_{∞} is this maximum reflectance. A little algebra leads to

$$\frac{K}{s} = \frac{(1 - R_{\infty})^2}{2R_{\infty}} \equiv f(R_{\infty})$$

which defines the Kubelka-Munk function or the remission function $f(R_{\infty})$. Keeping in mind that $0 \leq R_{\infty} \leq 1$, the above definition shows that $f(R_{\infty})$ decreases as R_{∞} increases. For the practical purposes of the present study, $f(R) = f(R_{\infty})$ where R is the measured reflectance. All the experimental specimens can be treated as having "infinite" thickness.

Even though the theory is based on diffuse incident flux, it can be shown (13) that a parallel beam at 60° from the normal satisfies the theory, since this gives the same average path through each layer dx . Experimentally, it has been found that for powdered samples (14) diffusion within the sample is complete so parallel incidence at any angle gives the same results as are obtained from the more restrictive conditions assumed in the above treatment. In contrast, for paper materials (15) the geometry significantly affects the reflectance because of orientation of the fibers.

It might again be noted that the K-M absorption coefficient, K , is not the same as the commonly used absorption coefficient in transmission experiments except in the limit of no scattering. The scattering coefficient is not so easily identified, but as it increases, so does R_{∞} . For particle sizes, small compared to the wavelength, one might expect the λ^{-4} dependence known as Rayleigh scattering and for large particles,

compared to the wavelength, the scattering would be expected to depend on reflection from the particle surfaces and be independent of the wavelength.

Taking the logarithm of the remission function gives

$$\log f(R_{\infty}) = \log K - \log s$$

so a plot of $\log f(R_{\infty})$ versus wavelength gives the plot of $\log K$ versus wavelength shifted in the ordinate direction by an amount $-\log s$ which is expected to be constant or, at worst, a slowly varying function of wavelength when the particle size is large compared to the wavelength. With this particle size limitation, the $\log f(R_{\infty})$ vs λ plot is expected to give a good representation of the absorption coefficient spectrum.

Kortum, Bram, and Herzog (16) have tested the K-M theory and have confirmed the ordinate shift for various particle sizes with little change in the shape of the spectrum for particle sizes $> \lambda$. They made transmission measurements on a didymium-glass filter and then ground the glass to various particle sizes upon which they made reflectance measurements. The transmission curve closely matches the remission function curves. They also found a linear dependence of scattering coefficient on grain size in this same region and determined absolute values for the scattering coefficient as a function of wavelength and particle size.

Wendlandt and Hecht (9) refer to an investigation of Kortum and Oelkrug (17) in which they relate the scattering coefficient to frequency as $s \propto \nu^{\alpha}$ where α is ~ 2.6 to 3.6 for average particle size $< \lambda$; ~ 1 for average particle size $\approx \lambda$; and ~ 0 to 1 for average particle size $> \lambda$. Blevin and Brown (18) have investigated scattering in suspensions

and concluded that the "optimum particle diameter for light scattering is approximately equal to the wavelength of the light in the particle, regardless of the matrix."

Another approach to the problem of relating optical parameters to diffuse reflectance uses a model in which the material is assumed to be composed of parallel layers and considers the reflection and absorption of these layers. Several of these statistical methods have been proposed (19, 20) with the one by Johnson (21) being typical and commonly referred to (9, 11, 12).

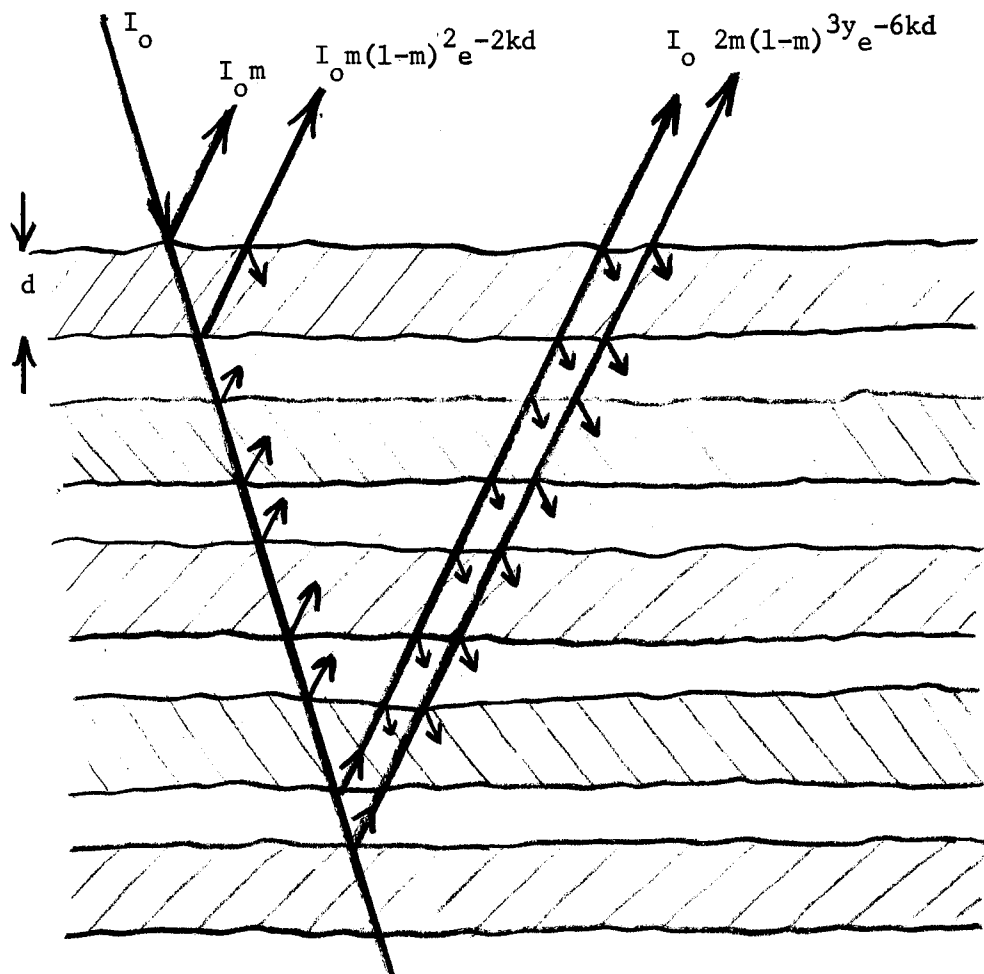


Figure 2. Johnson's Parallel Layer Model

With m being the fraction reflected at each surface encountered, and neglecting any upward reflection from previously reflected rays, any scattering, and any refraction, one can write for the reflected intensity

$$I = I_0 m + I_0 2m \sum_{p=1}^{\infty} (1-m)^{yp} e^{-2kpd}$$

where yp is the mean number of attenuating reflections which rays passing through $2p$ absorbing layers undergo, k in the conventional absorption coefficient, and d is the thickness of each layer (assumed to be the same as the diameter of the particles making up the layer). With some manipulation, including the formula for the sum of a geometric progression, one can arrive at

$$R = m \left[\frac{2(1-m)^y e^{-2kd}}{2kd-y \ln(1-m)} + 1 \right]$$

The quantity m is assigned a rather arbitrary value of 1.5 times that obtained from Fresnel's formula for normal incidence which corresponds to an average angle of incidence of around 30° and an index of refraction (n) in the range normally encountered, and y is determined by solving

$$\frac{(1-m)^{y-1}}{y} = \frac{1}{2} + \frac{1}{4} m + \frac{1}{6} m^2 + \frac{1}{8} m^3$$

which normalizes the reflectance equation, thus requiring $R = 1$ for $k = 0$. Normally y would be 4, but the above equation gives values less than 2. This process is intended to correct, at one time, for the ne-

glect of refraction, scattering and the discarded reflections mentioned earlier. The author gives graphs from which values of kd can be read if the reflectance and index of refraction are known. He limits the usefulness of this model to values of reflectance between 0.2 and 0.8 and his tests, using pulverized materials of known k , show good agreement with expected values.

Melamed (22) improved on Johnson's model by carrying out the summation over individual particle reflections. Since particle geometry must be known, a close packed array of spherical particles of diameter $d > \lambda$ is assumed to represent a randomly shaped and oriented arrangement of real particles. His general solution for the reflectance of a thick sample is

$$R_{\infty} = 2x \bar{m}_e + \frac{x(1 - 2x \bar{m}_e)T(1 - \bar{m}_e R_{\infty})}{(1 - \bar{m}_e R_{\infty}) - (1 - x)(1 - \bar{m}_e)T R_{\infty}}$$

where x is the fraction of the radiation which emerges from a particle and is scattered toward particles one particle distance closer to the surface. The evaluation of x assumes the close packing of spherical particles and small kd values. The quantity \bar{m}_e is an average reflection coefficient for the surface of a particle for externally incident radiation and its evaluation involves the Fresnel relations and assumes an ideal diffusing surface. The quantity T is the transmission of an individual particle and is evaluated from

$$T = (1 - \bar{m}_i) M / (1 - \bar{m}_i M)$$

with

$$M = 1 - \frac{2}{3} kd$$

and \bar{m}_i being an average reflection coefficient for internal radiation and is found much like \bar{m}_e .

The results again are published graphs relating R, kd, and index of refraction n, from which kd values can be read knowing the other quantities. The model was tested with a didymium-glass filter, as others have been, and shows good agreement between reflection and absorption methods.

Although Wendlandt and Hecht (9) and Simmons (23) consider the Melamed model to be the best yet, Johnson (24) argues that the dependence of R on n is incorrect and opposite that of his own model (21). However, Johnson admits that in the region of interest, $1.7 < n < 2.0$, the models compare favorably. Simmons (23), in a very recent publication, using a treatment similar to Melamed, has arrived at a very simple expression

$$R = e^{-[2n(\frac{kd}{3})^{1/2}]}$$

relating the parameters of interest, which have the same meaning as before. His result is based on the common assumptions of ideal diffuser, $d > \lambda$, infinite thickness, and uniform spherical particles. His success, however, comes from the assumption of small absorption, applied at two places in his treatment, and in such a manner that they tend to counteract each other, thus making the result applicable for kd values of, perhaps, 0.4 and smaller.

The following table compares kd values from the Johnson, Melamed, and Simmons models with the first two being taken from published graphs and the latter calculated. In all cases, n was taken to be 2.0 which is approximately correct for SnO₂.

The variation in the kd values given in this table confirms a belief of Johnson (24) who said "we do not believe that diffuse reflectance can

TABLE I

A COMPARISON OF kd VALUES FROM JOHNSON, MELAMED, AND SIMMONS MODELS

R Reflectance	kd		
	Johnson	Melamed	Simmons
.90	.017	.0028	.0021
.80	.035	.011	.0093
.70	.060	.033	.024
.60	.092	.051	.049
.50	.132	.085	.090
.40	.204	.153	.157
.30	.332	.370	.272
.20	.705	.686	.486

be relied on as a highly precise method of determining absolute absorption". He did feel it feasible to be within 50%, however.

In Figure 3 are plots of the K-M remission function and $(\ln R)^2$ from the Simmons model, versus reflectance, with the ordinate shifted to bring the high reflectance ends into coincidence. With n and d constant, $(\ln R)^2$ is proportional to the absorption coefficient in the Simmons model, and is seen, in the region above 30% reflectance, to give the same shape curve as the remission function which is proportional to the K-M absorption coefficient K . The justification of using the remission function in place of the absorption coefficient is now apparent even though it can't be identified as such. Absolute values of the absorption coefficient may contain great uncertainty but the shape of the absorption spectra will show excellent agreement between models if the other assumptions of the models are met; namely small values of kd and $d > \lambda$.

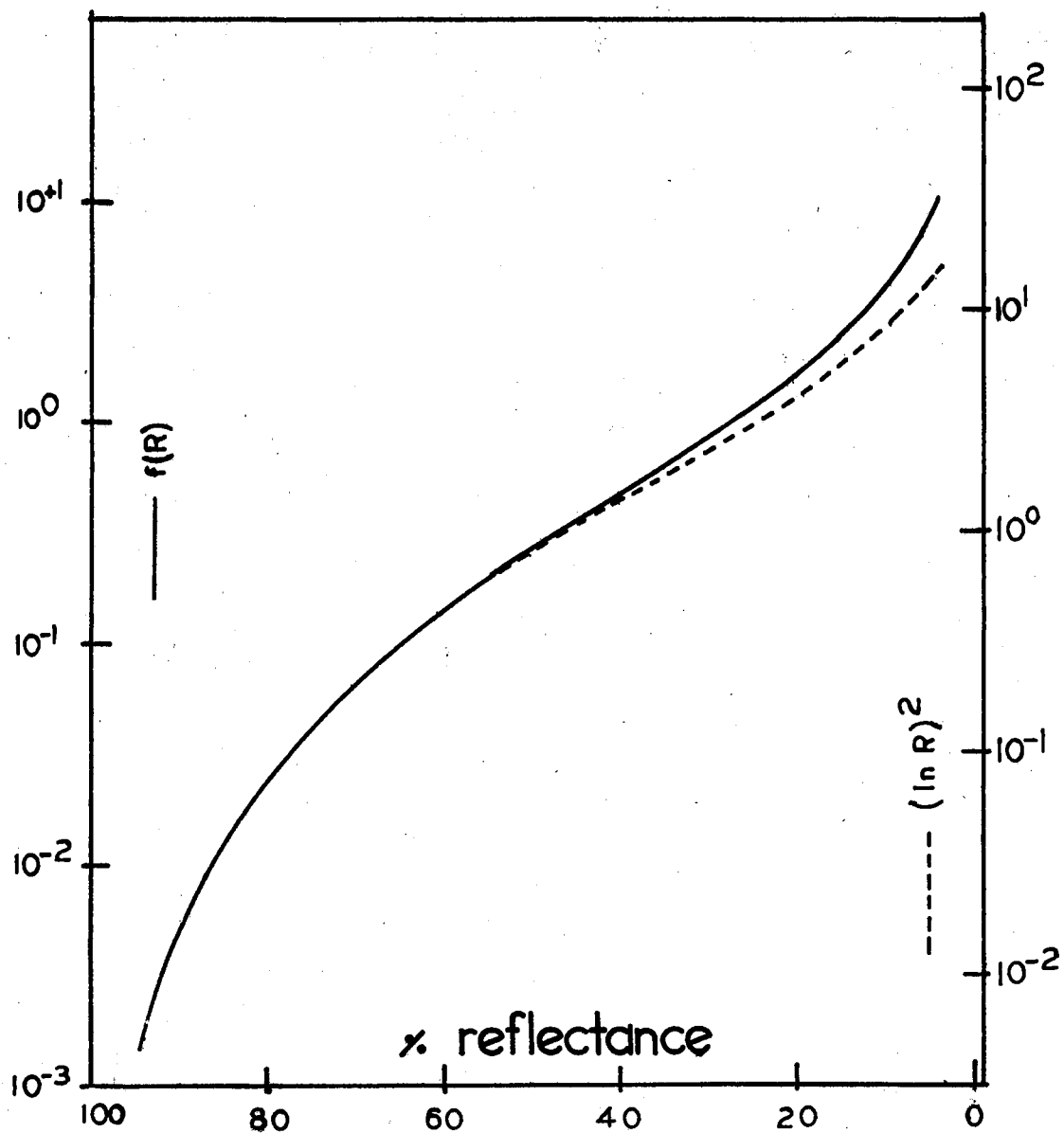


Figure 3. A Comparison of K-M Remission Function With the Absorption Coefficient From Simmons Model

CHAPTER III

INSTRUMENTATION AND EXPERIMENTAL DETAILS

Many flux averaging devices suitable for diffuse reflectance measurements have been proposed. Dunn (25) has designed and tested an ellipsoidal mirror reflectometer in which the sample and detector are at the foci of an ellipsoidal mirror. Derksen and Monahan (26) employed a hemispherical mirror and placed the sample and detector at conjugate points slightly displaced from the center of curvature and in a plane perpendicular to the optical axis of the mirror. Shibata (27) uses opal diffusing glass ahead of the sample and looks at the reflected light in a specific direction away from the combination.

The most widely used device and the one chosen for this work is the integrating sphere in which the inner surface of a sphere is coated with a "perfectly" diffusing material which assures that the illumination within it is uniform. The theory of the integrating sphere is old, but Jacquez and Kuppenheim (28) have recently covered the theory including errors due to holes in the sphere, method of use (comparison versus substitution), and flat as opposed to curved samples. Wendlandt and Hecht (9) have a chapter in their book on this subject and include coatings for the sphere. Hardy and Pineo (29) discuss errors while Olson and Pontarelli (30) examine asymmetries of spheres.

The various devices which incorporate integrating spheres can be classified as comparison, in which both the sample and a standard occupy

a part of the sphere wall at the same time; and substitution, in which the sample and standard occupy the same part of the sphere wall but at different times.

In the comparison case, the incoming beam falls first on the sample (or standard) and then on the other and it can be shown (28, 9, 29) that

$$\frac{B_s}{B_{st}} = \frac{r_s}{r_{st}}$$

where r_s and r_{st} are the reflectances of the sample and standard respectively, B_s and B_{st} are the radiant fluxes passing through a small hole to a detector upon illumination of the sample and standard respectively.

In the substitution case, the efficiency of the sphere changes as the sample is replaced by the standard so the illumination within the sphere is not directly proportional to the reflectance of the sample and standard. It can be shown (28, 9, 29) that

$$\frac{B_s}{B_{st}} = \frac{r_s}{r_{st}} \left\{ 1 - \frac{(r_{st} - r_s) \frac{c}{s}}{1 - \frac{rd}{s} - r_s \frac{c}{s}} \right\}$$

where r is the reflectance of the sphere coating, s is the area of the sphere, c is the area of the sample port, and $d = s - a - b - c$ where a is the area of the beam entrance port (or ports) and b is the area of the detector port. The quantity

$$\frac{(r_{st} - r_s) \frac{c}{s}}{1 - \frac{rd}{s} - r_s \frac{c}{s}}$$

is called the sphere error and occurs because of different efficiencies of the sphere when the sample and standard, respectively, are at the sample port. If the sample and standard are flat instead of being curved to fit the curvature of the sphere, then additional errors are introduced; this is at least an order of magnitude less than the previously discussed sphere error, but it does apply to both the substitution and the comparison methods (9).

The integrating sphere attachment, as designed for a Beckman DK-1 spectrophotometer, is shown in Figure 4. The sphere itself is formed from two spun aluminum hemispheres obtained from Weber Brass Company. This device replaces the lid to the sample compartment, with the 45° mirrors aligned so as to cut the sample and reference beams and direct them to the openings in the top of the sphere where the standard and reference samples will be located. In the normal operation of the DK-1, the sample beam undergoes two reflections at the hands of the beam splitting mechanism before entering the sample compartment and the reference beam undergoes two reflections after leaving the sample compartment in the process of putting the two beams back together prior to sending them to the detectors. By interrupting this process with mirrors in the sample compartment, the reference beam thus undergoes one reflection before striking the reference material and the sample beam undergoes three reflections before striking the sample material. It was intended that the device would operate as a comparison sphere, but the sample beam undergoes two more reflections than the reference beam, and aluminized mirrors have a selective absorption centering on 850 mμ (31). The illumination of the sphere by the sample beam is therefore less than that of the reference beam near 850 mμ, so true double beam operation is not

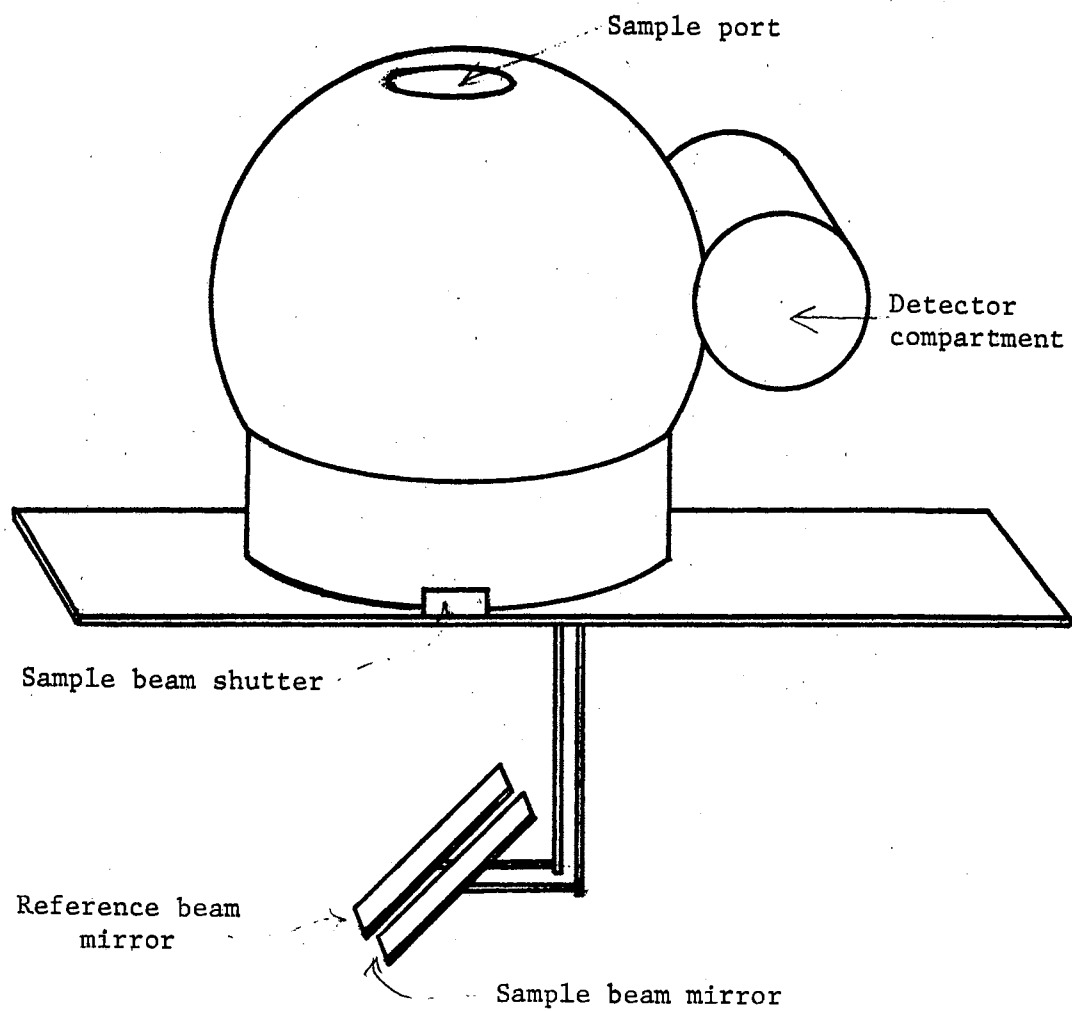


Figure 4. Integrating Sphere Attachment for D-K 1 Spectrophotometer

possible. If matched mirrors are available, then two additional reflections can easily be built into the reference beam to achieve true double-beam operation. Some advantage was gained over single beam operation; however, as less instability and drift are to be expected (32). Data were taken with a roughened aluminum disk in the reference location to reduce the difference between the two beams. The reference and then the sample were run in the sample location, thus operating the sphere in the substitution mode. The actual operation of the sphere will be elaborated on later.

The cylinder on the right of the sphere in Figure 4 houses the detectors. In the IR range a B3-SA22 lead sulfide detector from Infrared Industries, Inc., was used. In the visible range a 1P28 photomultiplier was used. With both detectors, power supplies external to the spectrophotometer were used and the signal prepared for injection into the DK-1 preamplifier at test point A (33). The signal strength from these two detectors was approximately equal at 800 m μ so this was chosen as the crossover point.

Many materials and methods of application have been proposed for standards and the coating of integrating spheres. Budde (34) considers the effect of surface texture, particle size, purity, and surface thickness on the reflectance of BaSO₄ paints. Middletown and Sanders (35) propose the use of carboxymethyl-cellulose as a paint binder and give the reflectance of both BaSO₄ and MgO paints prepared this way. The MgO paint has absorptions at 1.4 and 1.9 μ which they attribute to water incorporation. Other paint formulations are discussed in Scientific Papers of the Bureau of Standards #474. (36) Brandenburg and Neu (37) have studied the directional reflectivity of MgO and BaSO₄ and found that both

deviate from the ideal diffuser described by the Lambert cosine law. Dunn in N.B.S. Circular #279 (25) suggests the spraying of a BaSO_4 -benzene slurry onto a surface coated with a benzene soluble contact cement. Middleton and Sanders (38) have studied the reflectance of MgO in the visible range as a function of the method of preparation, aging, and U.V. irradiation. They found the preparation method to have a small effect; but more significant was reduction of about 1% in the blue region with time. They later extended their work to the I.R. (39) and found a sample several days old develops absorption bands at 1.4, 1.9, and 2.35μ . They suspect this is due to water and the formation of brucite (MgOH). Even though the ASTM has adopted a smoked MgO surface as a reflectance standard (40) they admit that age and method of preparation are problems. McAloren (41) reports an improved method of preparing reproducible MgO standards resulting in high uniform reflectance from 0.3μ to 2.6μ . He also found that if the powder bed is compacted, blue reflectance is uniformly decreased and that severe absorption bands at 1.4μ and 1.9μ occur.

The MgO standard used in this study was prepared by burning short lengths of Mg ribbon under a shallow aluminum cup. It was decided to accept the possibility of some aging and thus avoid variations in preparation. No absorption bands at 1.4μ or 1.9μ were observed.

For the sphere coating, a sprayed BaSO_4 -benzene slurry on rubber cement was attempted with a small laboratory freon-12 propelled unit. The results were unsatisfactory as benzene does not wet the BaSO_4 particles so they tend to clump together. If an equal portion of acetone is added, the slurry is smooth, sprays easily, and dries rapidly. The rubber cement coated hemisphere was heated slightly with a lamp before and be-

tween applications of the slurry and unusually rough areas were smoothed with a soft brush between applications. The resulting coating was durable (more so than smoked MgO surfaces) and fairly smooth.

With the sphere thus constructed and coated, and with the roughened aluminum disk in the reference position, a reflectance spectra, with the MgO standard in the sample position, was made. The MgO was then replaced by a sample and its reflectance spectra, versus the aluminum disk, was made. These are both comparison spectra; so are thus described by the equations

$$\frac{B_{st}}{B_{Al}} = \frac{r_{st}}{r_{Al}}$$

and

$$\frac{B_s}{B_{Al}} = \frac{r_s}{r_{Al}}$$

where r_{Al} is not the true reflectance of aluminum, but an effective reflectance because of the difference in the optical paths previously noted for the sample and reference beams.

In any case, r_{Al} is a constant for all spectra made; so by dividing the above equations

$$\frac{B_s}{B_{st}} = \frac{r_s}{r_{st}}$$

which says that even though the method used is a combination of comparison and substitution modes, the result is equivalent to the comparison mode and the sphere error, due to changes in the composition of the sphere wall, is effectively zero. This same result can be seen by

realizing that in the normal operation of the DK-1, the electronics of the instrument adjusts the slit width (and thus the light intensity entering the sphere) to keep the electrical signal constant when the beam is on the reference channel. Any reduction in sphere efficiency would therefore be counteracted by an increase in light intensity entering the sphere, making the effective sphere efficiency a constant.

So that the reflectance of samples could be determined after various treatments, a vacuum chamber with a provision for mild heating of the sample was designed and constructed to fit over the sample port of the sphere. A quartz window covered both the standard and the sample during measurements and a copper-constantan thermocouple monitored the temperature of the copper slab to which the sample was attached. For the purposes of analysis of the data obtained in this fashion, the corrections necessitated by the presence of the quartz windows have been assumed negligible.

The samples were prepared from reagent grade SnO_2 (Fisher, lot 754993). They were pressed into 5 gram, 1 inch diameter disks by a pressure of 7,900 psi in a steel die. The samples were fired by placing them in a cold, electric glowbar furnace, which was then raised to a specified temperature as quickly as possible. The disks were removed when hot, after a specified time, and allowed to cool in air. Table II summarizes these treatments.

Sample #4 is doped with 0.7% ZnO by mixing the materials in an acetone slurry, agitating for 24 hrs., and then air drying before pressing.

While firing sample #8, the temperature rose to 1440°C for a short time, approximately 4 hours, at which time the fuse blew. The sample

TABLE II
 SAMPLE PREPARATION TREATMENTS

Sample No.	Max. Temp.	Time to reach max. temp.	Time at max. temp.	Total firing time
1	----- not fired -----			
2	1240°C	14 hrs.	4 hrs.	18 hrs.
3	1240°C	14 hrs.	30 hrs.	44 hrs.
4*	1240°C	14 hrs.	70 hrs.	84 hrs.
5	1240°C	14 hrs.	96 hrs.	110 hrs.
6	1400°C	19 hrs.	6 hrs.	25 hrs.
7	1400°C	19 hrs.	22 hrs.	41 hrs.
8*	1400°C	19 hrs.	31 hrs.	50 hrs.

* See Page 23.

slowly cooled in the furnace to 200°C in 12 hours, which is not included in the time shown in Table II.

Preliminary reflection measurements indicated that no significant change resulted from grinding and cleaning the sample surfaces; so, with the exception to be noted later, data were taken on the samples as they came from the furnace.

CHAPTER IV

EXPERIMENTAL RESULTS

The integrating sphere thus constructed was used in the comparison mode to make spectra of both the samples and the MgO reference relative to a roughened Al disk. From these chart paper spectra (as directly produced by the spectrophotometer) values of the reflectance were read for a particular wavelength and then divided to give B_s/B_{st} which has been shown to be equivalent to r_s/r_{st} . Thus, a reflectance spectra of the sample relative to the standard is generated point by point.

In Figure 5 a comparison of the effect of firing at two different temperatures is made with the results from an unfired sample. Note the crossing of the curves in the IR and the appearance of the shoulder near 550 μ .

In Figures 6 and 7 the effect of firing time at both temperatures is observed.

In Figure 8 the effect of doping with 0.7% ZnO is observed.

For use in the vacuum chamber a sample, having been given the same firing treatment as #2 (henceforth noted as 2*), namely 1240°C for 18 hours, was ground on both sides enough to make them flat. This sample was then cleaned in acetone with an ultrasonic cleaner and cemented to the copper slab on the end of the vacuum chamber heater using a thin layer of vacuum epoxy.

In Figure 9, the effect produced by exposing 2* to a mercury lamp

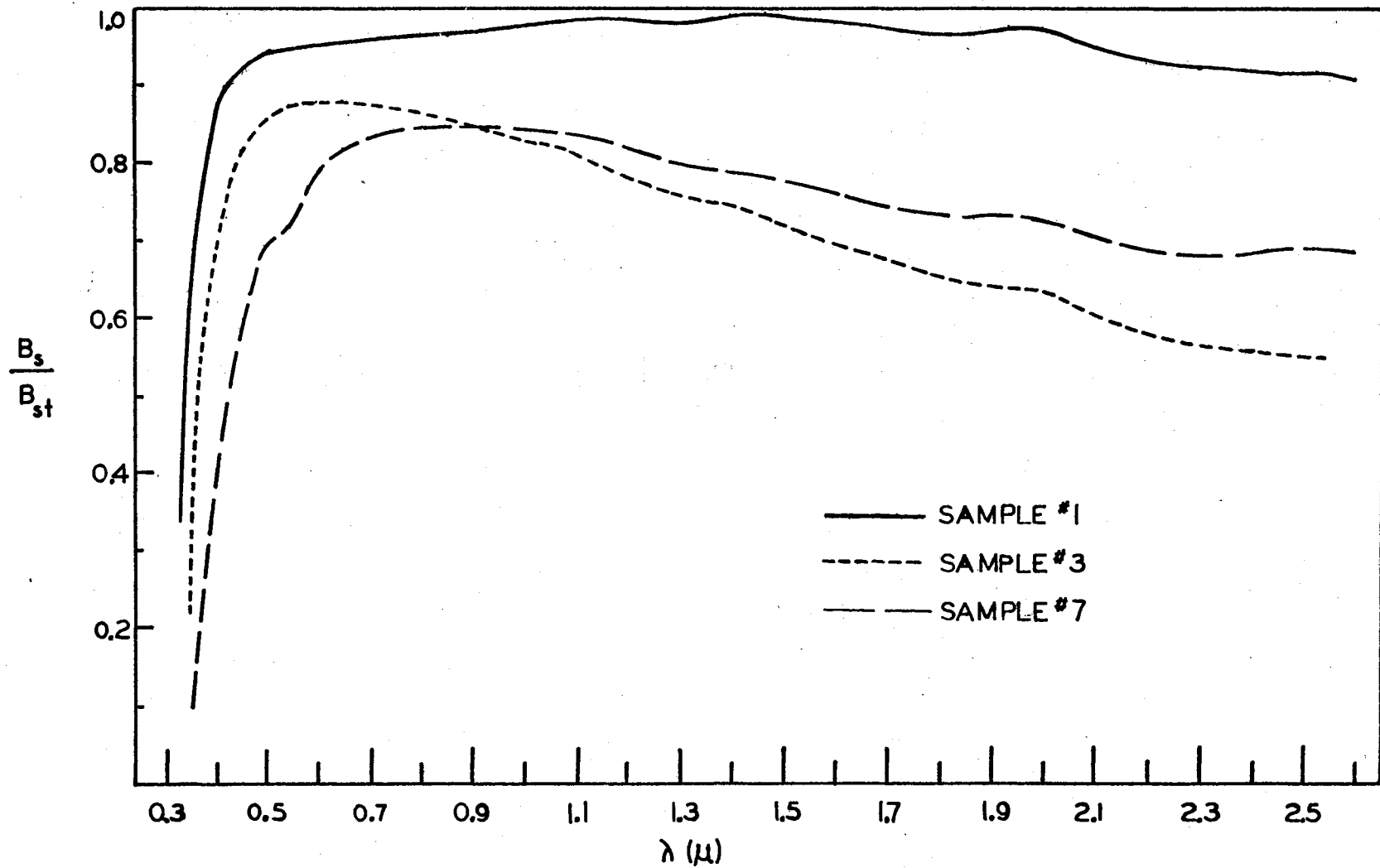


Figure 5. Effect of Firing Temperature on the Relative Reflectance

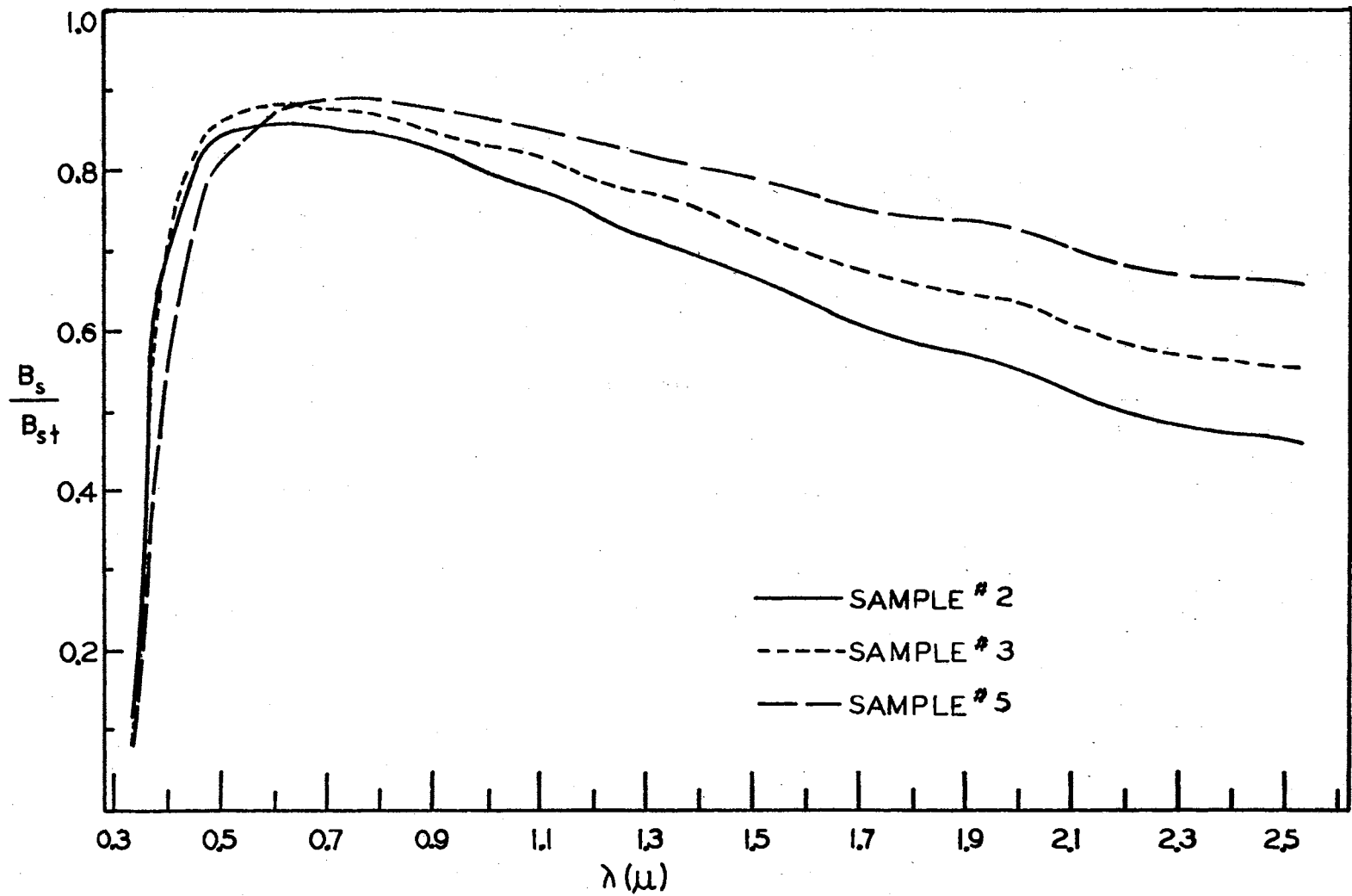


Figure 6. Effect of Firing Time at 1240 °C on the Relative Reflectance

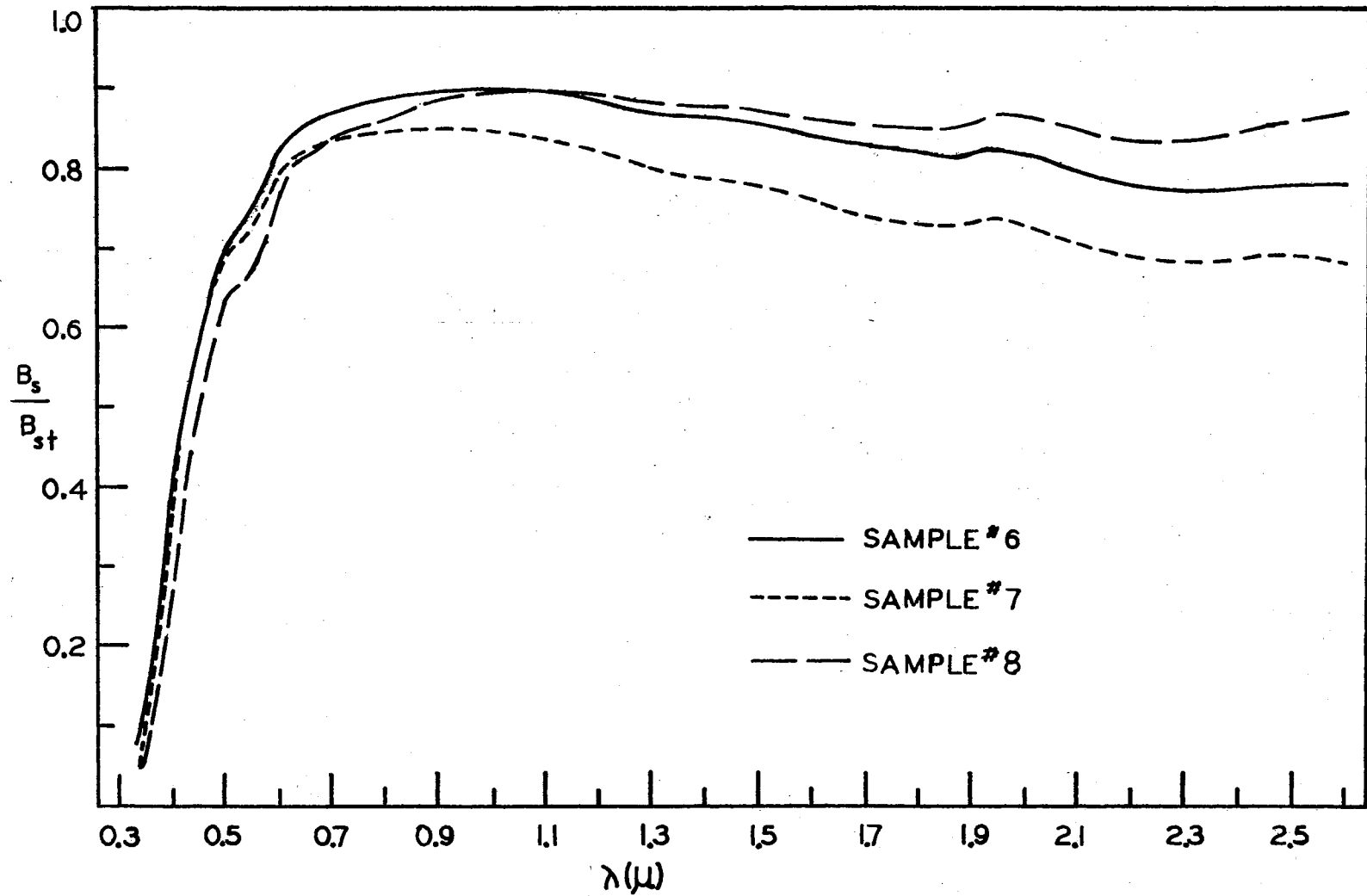


Figure 7. Effect of Firing Time at 1400 °C on the Relative Reflectance

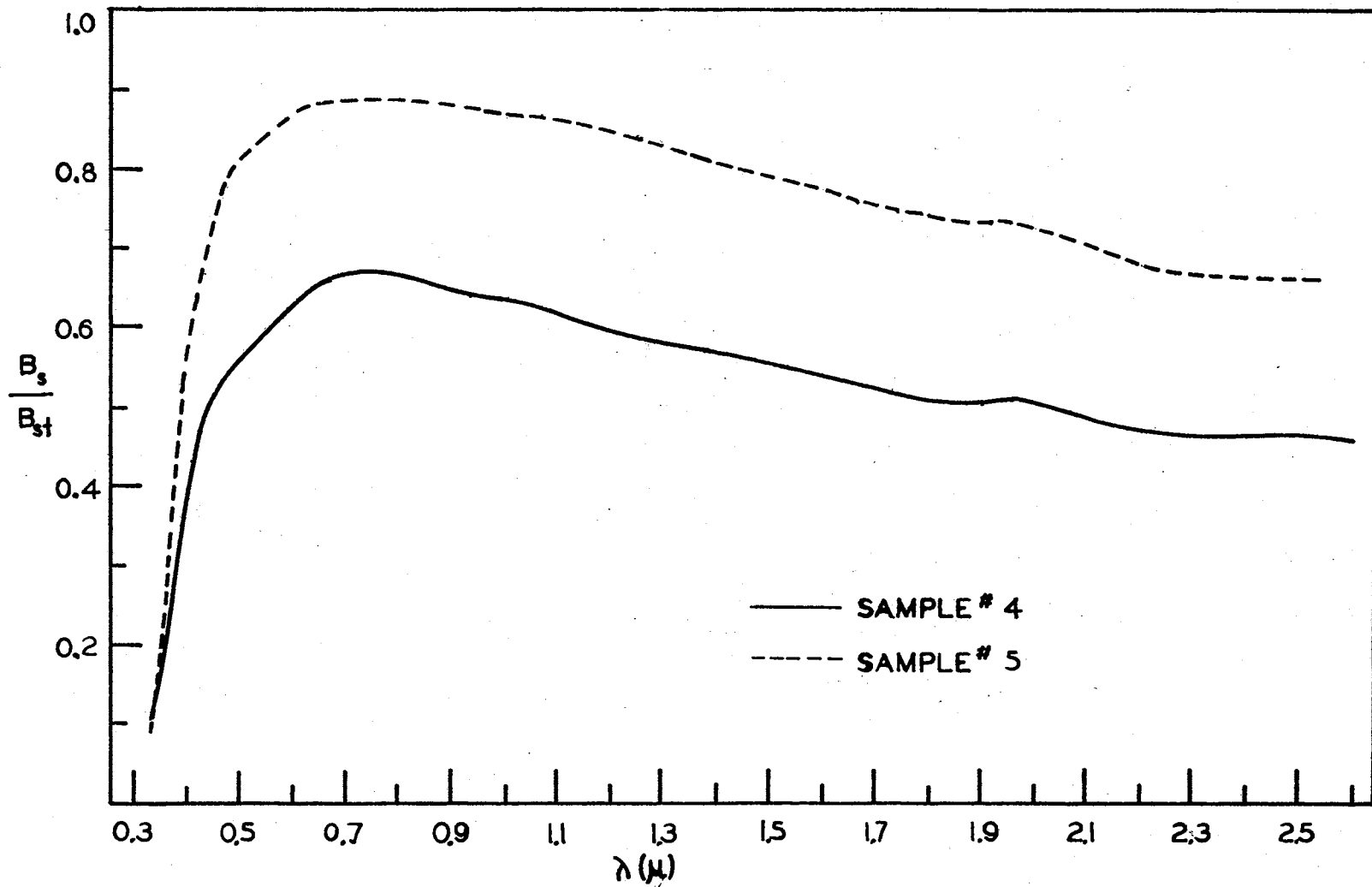


Figure 8. Effect of Doping With 0.7% ZnO on the Relative Reflectance

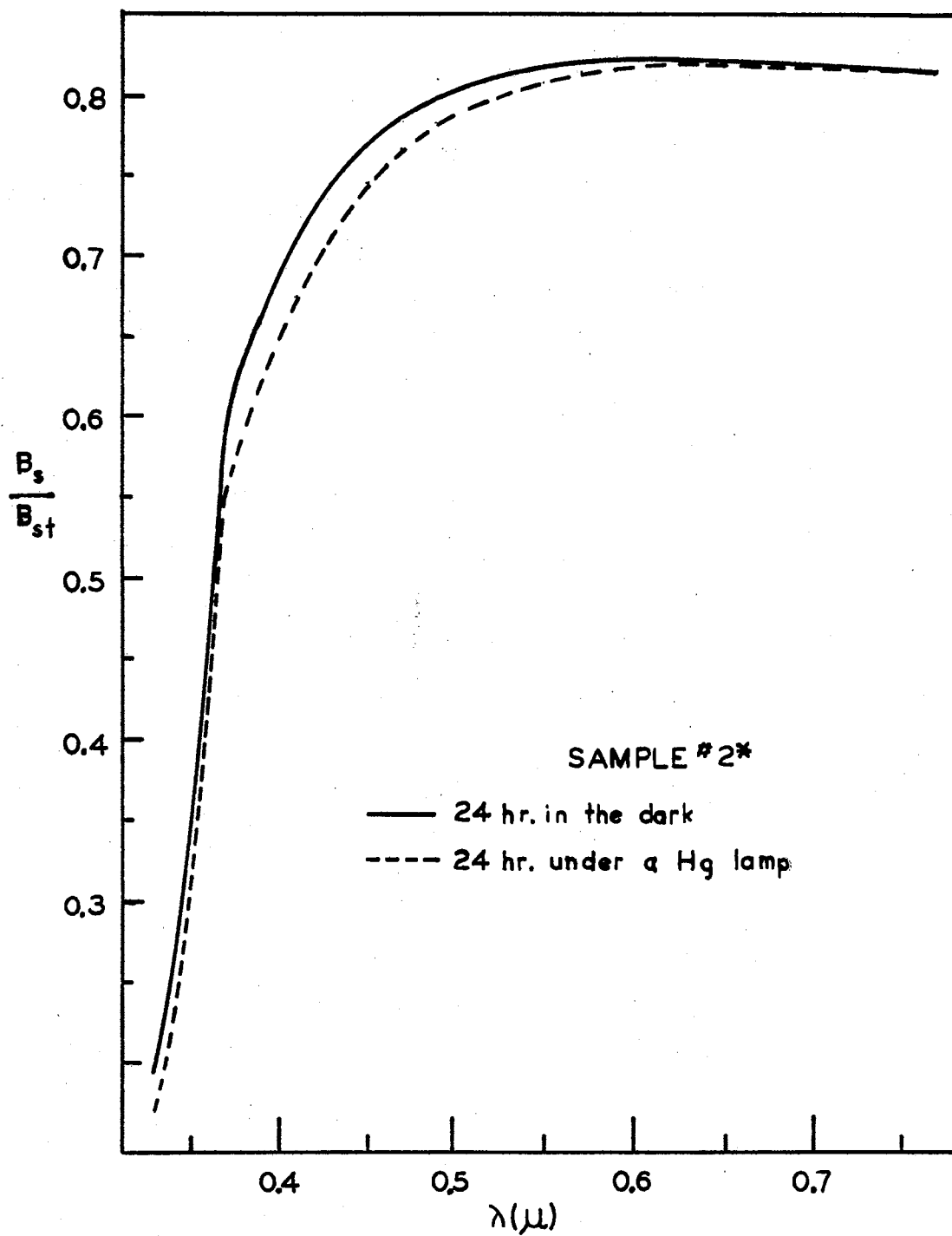


Figure 9. Degradation of the Relative Reflectance With U-V Light

for 24 hours in air, after being kept in the dark for 24 hours is seen. Although the effect is small, it is reproducible with all samples and even detectable visually as a slight yellowing of the sample. No significant change occurs in the IR region. A similar effect results from exposure to ordinary florescent light. In all cases, however, recovery is incomplete over a period of a few days.

In Figure 10 the shift in the apparent absorption edge due to mild heating of the sample is seen. Recovery from this treatment is complete. The remainder of the spectrum is unaffected.

Attempts were made to detect the chemisorption of oxygen by changes in reflection. Mild heating in N_2 and O_2 as well as vacuums below 10μ were used but no significant change in reflectance was observed.

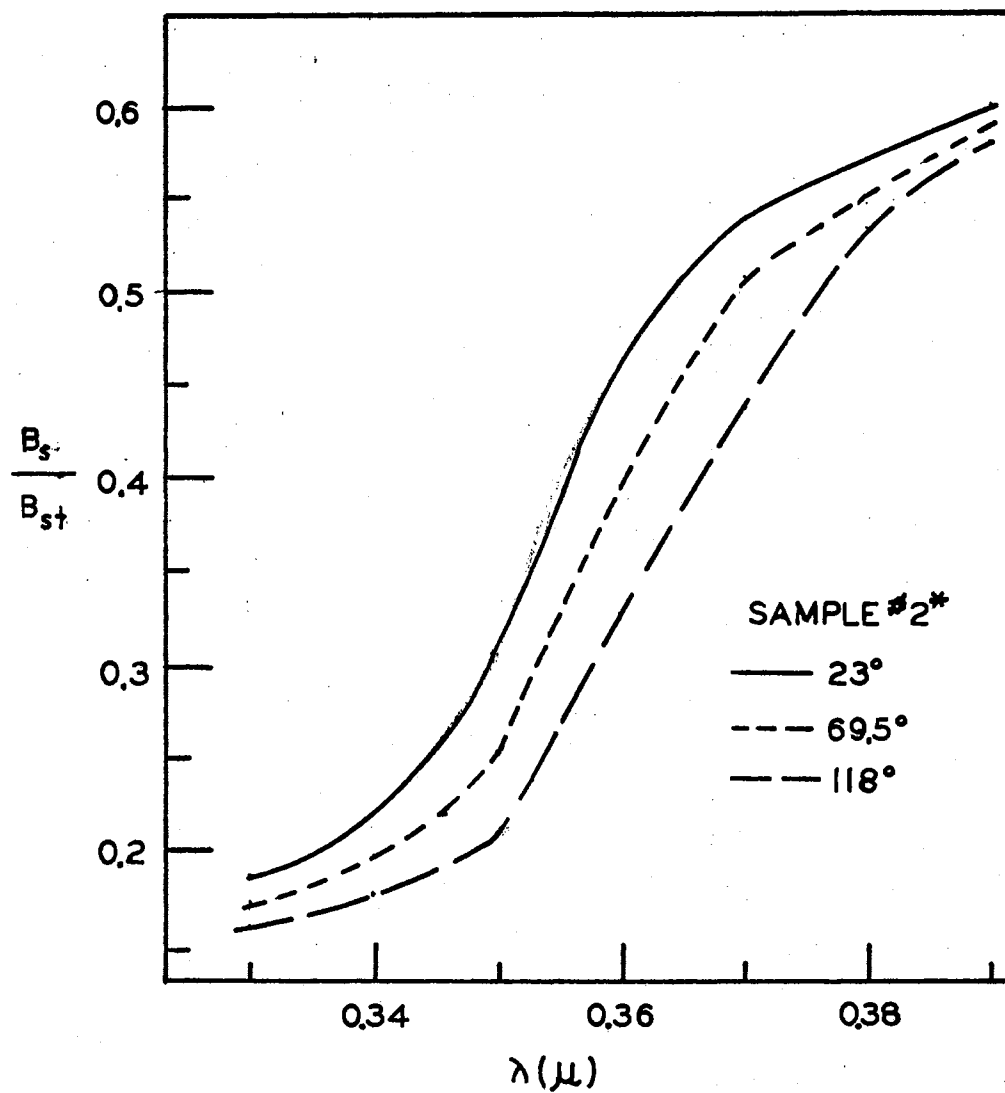


Figure 10. Temperature Shift of Absorption Edge

CHAPTER V

CONCLUSIONS

In an earlier study, Rutledge (42) found the grain size of Fisher certified reagent SnO_2 powder to be 0.5 microns by nitrogen absorption techniques. Matthews (43), using photographic techniques, found pure SnO_2 fired to 1175°C for four hours, to have one micron grains and when fired to 1460°C for four hours to have five micron grains. Clearly the grain size increases upon firing and with the firing temperature and longer firing times would be expected to further increase the grain size. Matthews (44) earlier found the density of the ceramics to increase with both firing time and temperature.

Schatz (45, 46) studied the effect of pressure on the spectral reflectance of many materials. He concluded that for transparent particles, especially white oxides, a large decrease of reflectance occurs with increasing pressure. His proposed explanation was that compaction decreases the space between particles and therefore reduces the total internal reflection that occurs, thus increasing transmission of the material. It can be shown that radiation can propagate across a thin film of low index of refraction material that is between higher index of refraction materials even though the angle of incidence at the first surface exceeds the critical angle (47). This effect increases with wavelength, is known as frustrated total reflection, and justifies Schatz's explanation. Schatz (45, 48) also studied the effect of sin-

tering temperature on the reflectance of several metal oxides. His conclusion, of significance here, was that actual sintering would also result in a decrease in the distance between particles and thus a decrease in reflection.

Keeping in mind that the scattering contribution to the reflection is wavelength-dependent and is a maximum when the particle size matches the wavelength, a possible explanation of the qualitative reflectance changes observed in Figures 5 through 7 can be proposed.

Presumably, two simultaneous competing effects are occurring. As sintering begins, compaction results and the overall reflectance decreases. The longer wavelengths would experience the frustrated total internal reflection to a greater extent, so the reflectance in the IR would decrease the most because these wavelengths penetrate further into the sample. With either increased firing time or temperature, the effect would be increased as greater compaction would occur. At the same time, the average grain size is increasing from a low of 0.5 microns. Therefore, the region in the spectrum where the maximum contribution from scattering occurs, is moving out into and through the IR range. This will tend to increase the IR reflection. It is felt that the compaction process is relatively rapid as compared to the increasing grain size process so that the first effect observed is a decrease in reflection. The combination of these processes is observed to always reduce the reflection below that of the powdered sample.

Many authors have used reflectance or transmission experiments on crystalline slabs, from which absorption coefficients can be found, to determine the absorption edge in semi-conductors and thus the band gap. Moss (49) defines the absorption edge "as the point where the slope of

the absorption coefficient is a maximum" and then goes on to show that this corresponds to the point where the absorption coefficient is half its short wavelength value. He uses this well known $\lambda_{\frac{1}{2}}$ point to obtain the energy gap.

Fochs (50) found that the diffuse reflection spectra from semiconductors plotted versus decreasing photon energy shows a linear increase in the neighborhood of the absorption edge and he uses the onset of the linear region, on the short wavelength side, to define the absorption edge. The criteria of Moss and Fochs appear to be essentially equivalent.

The shape of the main absorption edge depends on whether the direct optical transition is allowed or forbidden. Indirect or phonon-assisted transitions may also affect the absorption edge shape, particularly at its lower photon energy end. Because of limited data, only a modest attempt could be made at searching for an energy gap value and emphasis was placed on the allowed direct transition analysis in view of the results of Summitt, Marley, and Borelli (3) on SnO_2 single crystals.

McLean (51) developed a theory for the absorption coefficient dependence on energy in direct transitions and Karvaly and Hevesi (52) use this method in their study of the diffuse reflectance spectra of vanadium pentoxide powder, with good results. For an allowed direct transition, the absorption coefficient varies as $[\text{h}\nu - E_g]^{\frac{1}{2}}/\text{h}\nu$ and for a forbidden direct transition, as $[\text{h}\nu - E_g]^{3/2}/\text{h}\nu$ where E_g is the band gap.

Smith (53) develops a simpler result, namely $k \propto (\text{h}\nu - E_g)^{\frac{1}{2}}$ for allowed direct transitions and $k \propto (\text{h}\nu - E_g)^{3/2}$ for forbidden direct transitions, but states his results are valid only for a limited range of $\text{h}\nu$ values. For the range of $\text{h}\nu$ values around $\text{h}\nu = E_g$, these expressions

are in reasonable agreement with the formulation of McLean. Lyashenko and Miloslavskii (5) use the simpler result in their analysis of thin SnO_2 films, while Summitt, Marley, and Borelli (3) also use the simpler form in their analysis of SnO_2 single crystals.

For this study, the absorption coefficient must be replaced by a quantity proportional to it. The K-M remission function is proportional to the K-M absorption coefficient which has previously been shown to be identifiable with the traditional absorption coefficient. Karvály and Hevesi (52) used this type of substitution in the visible range to analyze their vanadium pentoxide spectra. However, the Simmons model says that $(\ln R)^2$ is proportional to the absorption coefficient and it was decided to test this approach rather than one based on the K-M remission function. Since, as we have seen, $\frac{r_s}{r_{st}} = \frac{B_s}{B_{st}}$ with r_{st} being very nearly a constant, we can conveniently use $\frac{B_s}{B_{st}}$ in place of R leaving

$$\left[\ln \frac{B_s}{B_{st}} \right]^2 \propto \frac{[h\nu - E_g]^{1/2}}{h\nu}$$

for allowed direct transitions. Now, if a plot

of $\left[\left(\ln \frac{B_s}{B_{st}} \right)^2 h\nu \right]^2$ versus $h\nu$ shows a linear portion, an allowed direct transition is assumed to occur with the straight line intercepting the energy axis at E_g .

Figure 11 shows plots of relative reflectance versus photon energy for samples #1 and #8. Using the criterion of Fochs, sample #1 shows a band transition of around 3.65 eV whereas sample #8 shows its first linear increase at 3.6 eV. Since polycrystalline materials have random crystal orientations and since unpolarized light is used, this energy can represent only an "effective" energy gap weighted by the two propa-

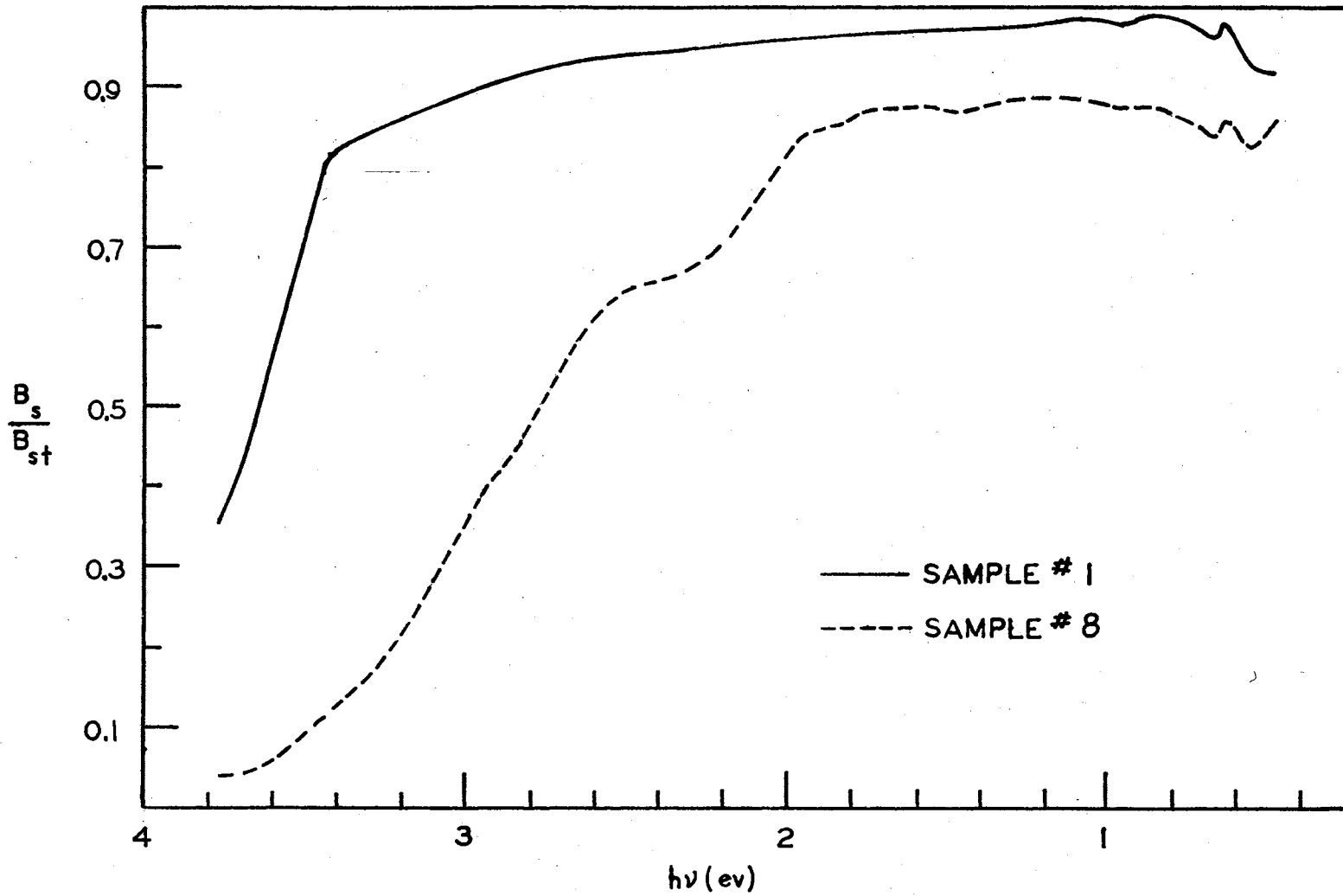


Figure 11. Relative Reflectance Versus Photon Energy

gation possibilities, $E // C$ and $E \perp C$.

Sample #8 shows a slight shoulder at 2.9 ev, a very apparent shoulder near 2.2 ev, and other less certain features at 1.8 ev, 1.4 ev, and 0.95 ev, where sample #1 also shows a slight reflectance dip. Both samples indicate a more distinct change at 0.65 ev while sample #8 has an additional dip at 0.55 ev. It should be noted that the curve of sample #1 was drawn through some slight variations in reflectance in a smooth manner, as these variations were deemed to not be resolved sufficiently to be shown.

The reflectance changes described above are thought to be associated with absorption transitions arising from the presence of impurity or other defect states in the forbidden gap. The density of these states, and thus the absorptions associated with them, might well be a function of the firing conditions. This is a possible explanation for the continued reduction in relative reflectance of the higher energy half of the visible spectrum as seen in Figures 5 through 7. Other evidence for a transition at 2.2 ev comes from visual observation of the samples as they are removed from the furnace. As they cool, there is a persistent, distinctive, yellow emission from all samples. The eye interprets, as a yellow color, a narrow band of wavelengths centered around 0.580 microns. An electronic transition from the conduction band into a level 2.15 ev below this would account for such a color. This is probably due to a recombination process in which electrons drop from the conduction band into a level 2.2 ev below this band as cooling occurs.

The graphical methods that are based on the shape of the short wavelength side of the absorption edge cannot be used very successfully or reliably here, as the data in this region are very limited in the present

study and the reflectance is low enough to place the Simmons model in question. However, Figure 12, which is based on this method, does give an indication of an absorption edge energy of 3.42 eV which is roughly 5% less than the E₁C direct gap determined on single crystals by Summitt, Marley, and Borelli (3). This is probably fortuitous.

Data from the SnO₂ powder shows a relative reflectance of 0.65 at 0.35 microns wavelength. Using the Simmons model and assuming the grain size to be 0.5 microns and the index of refraction to be 2.0, we calculate the absorption coefficient to be $2.1 \times 10^3 \text{ cm}^{-1}$. This calculation is sensitive to grain size and doesn't really fit the Simmons model, which as we have noted, assumes λ to be much smaller than the particle size. The result is, however, near the range that would be expected for allowed transitions.

Figure 10 shows the temperature shift of the reflectance spectra. Taking a relative reflectance of 0.30, which is a reasonable estimate of the start of the absorption edge, an estimate of the absorption edge temperature shift is found to be $-8.7 \times 10^{-4} \text{ eV/}^\circ\text{K}$. Again, this is in acceptable agreement with several values quoted in Chapter I.

Finally, the reduction in reflection seen in Figure 9, due to exposure to radiation from a mercury lamp, cannot yet be explained. Similar optical degradation effects have been reported by others, however. Filimonov (54) reports a reduction in the overall transmission of an SnO₂ thin film when exposed to mercury lamp radiations and shows that partial recovery results when oxygen is allowed to surround the sample. A comparable recovery was never indicated in this study. The Lockheed Palo Alto Research Laboratory (55) found that a reduction in both the visible and IR reflectance of ZnO ceramics occurred upon exposure to

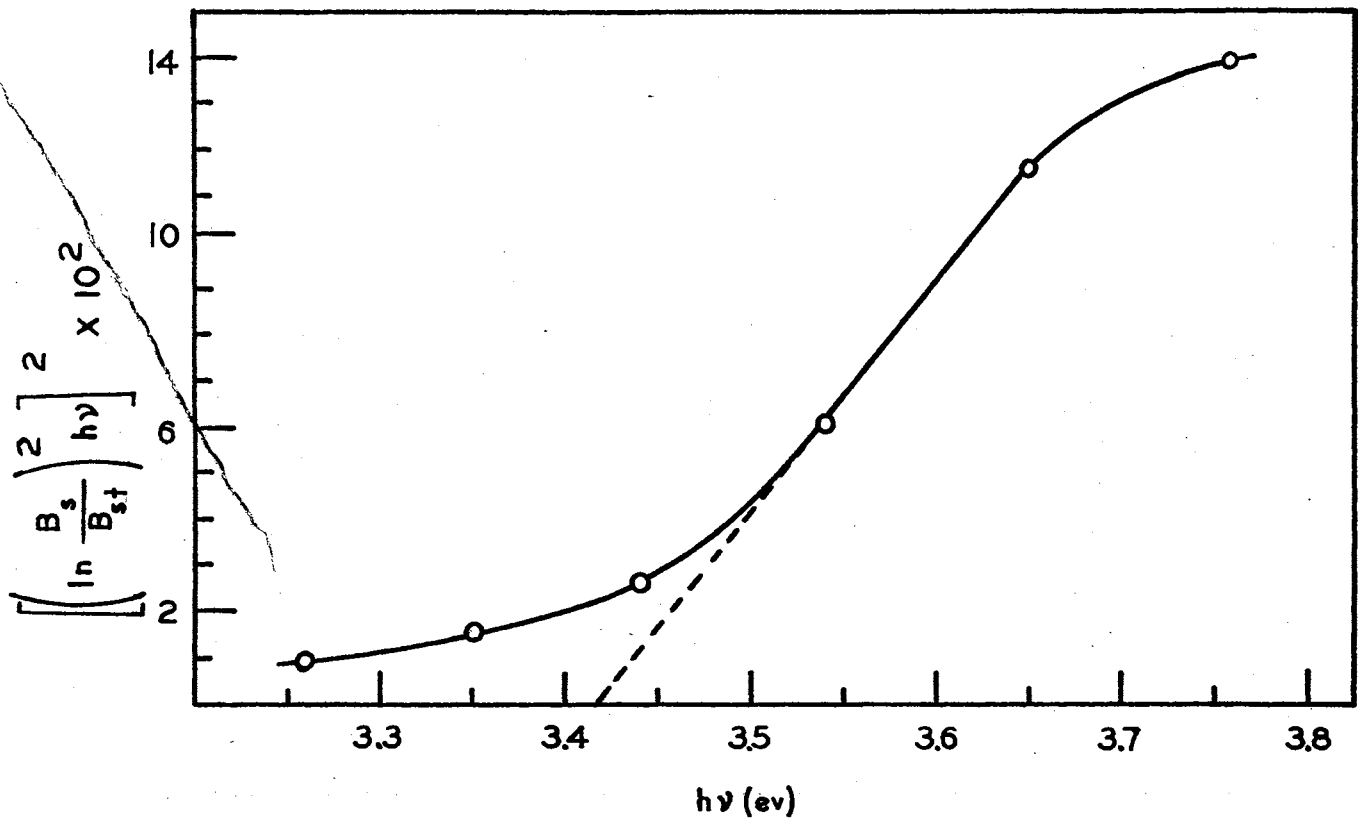


Figure 12. Extrapolation to Find an Allowed Band Transition

solar radiation. The IR recovered upon exposure to oxygen but the visible range damage never recovered.

In Figure 8 a reduction in reflection across the entire spectrum due to doping with 0.7% ZnO is seen. Moss (49) says that impurity absorption in impure semi-conductors may appear as a wide continuum extending to energies as great as those of the main absorption edge. Thus impurity absorption can account for at least part of the overall reduction observed.

It has been shown in this study that with relatively simple techniques, polycrystalline materials can yield the same type of information as single crystals with, however, less precision in many cases. Several possibilities for further study naturally suggest themselves. For example, if the short wavelength region could be extended and more data generated (by sweeping the wavelength more slowly while the chart speed remains the same) in the same region, then a better measure of the band gap and its variation with temperature might be achieved.

Some of the polycrystalline SnO₂ samples prepared by Matthews (44) had pink or blue colors. Every attempt to intentionally duplicate such colors failed; however, a few samples had tiny blue spots on them as though a small particle of impurity fell on the surface and produced the color during firing. One sample shattered during firing and a large piece fell between the fire brick and the furnace mantle. This fragment had a uniform blue color which indicates that an impurity from the mantle was the likely cause of the blue color. Intentional doping with various materials to produce colored samples would make an interesting optical study.

High speed spectrographic studies of the emissions from a cooling

sample right out of the furnace might also yield interesting information on recombination processes.



RECOMBINATION OF ELECTRONS AND HOLES

From Band

of 7.5 eV band

1000000

1000000

1000000

SELECTED BIBLIOGRAPHY

- (1) Summitt, Robert and N. F. Borelli, "Infrared Absorption in Single Crystal Stannic Oxide", J. Phys. Chem. Solids 26, 921 (1965).
- (2) Houston, Jack E. and E. E. Kohnke, "Photoelectronic Analysis of Imperfections in Grown Stannic Oxide Single Crystals", J. Appl. Phys. 36, 3931-3938 (Dec. 1965).
- (3) Summitt, R., J. A. Marley, and N. F. Borelli, "The Ultraviolet Absorption Edge of Stannic Oxide", J. Phys. Chem. Solids 25, 1465 (1964).
- (4) Wagasawa, M. and S. Shionoya, "Temperature Dependence of the Fundamental Optical Absorption Edge in Stannic Oxide", J. Phys. Soc. Japan 30, 1118 (1971).
- (5) Miloslavskii, V. K. and S. P. Lyashenko, "Study of the Optical Properties of Tin Dioxide Thin Films in the Visible and Ultraviolet Regions", Opt. Spectry. (USSR) 19, 55-8 (July, 1965).
- (6) Kohnke, E. E., "Electrical and Optical Properties of Natural Stannic Oxide Crystals", J. Phys. Chem. Solids 23, 1557-1562 (1962).
- (7) Ishiguro, Sasaki, Arai, and Imai, "Optical and Electrical Properties of Tin Oxide Films", J. Phys. Soc. Japan 13, 296 (March 1958).
- (8) Kubleka, P. and F. Munk, "Reflection Characteristics of Paints", Z. Technical Physik 12, 593 (1931).
- (9) Wendlandt, W. Wm. and Harry C. Hecht, Reflectance Spectroscopy, John Wiley and Sons, Inc., New York, 1966.
- (10) Kortum, G., Reflectance Spectroscopy, Berlin, Springer-Verlag, 1969.
- (11) Companion, A. L., "Theory and Application of Diffuse Reflectance Spectroscopy", Developments in Appl. Spectroscopy 4, 221-233 (1965) Plenum Press, N.Y.
- (12) Wendlandt, W. Wm., ed. "Modern Aspects of Reflectance Spectroscopy", Proceedings of A.C.S. Symposium on Reflectance Spectroscopy, 1967.

- (13) Kubella, Paul, *J. Opt. Soc. Am.*, 38, Part I 448 (1948); errata 38, 1067 (1948).
- (14) Kortum, G. and G. Schreyer, "On the Validity of the Kubelka-Munk Function for Reflection Spectra of Powders", *Z. Naturforsch* 11a, 1018 (1956).
- (15) Stenius, A. S., "Influence of Optical Geometry and Absorption Coefficient on Diffuse Reflectance Values", *J. Opt. Soc. Am.* 45, 727 (Sept. 1955).
- (16) Kortum, G., W. Braum, and G. Herzog, "Principles and Techniques of Diffuse Reflectance Spectroscopy", *Angewandte Chemie* 2, 333 (July, 1963).
- (17) Kortum, G. and D. Oelkrug, "The Scattering Coefficients of the Kubelka-Munk Theory", *Z. Naturforsch* 19a, 28 (1964).
- (18) Blevin, W. R. and W. J. Brown, "Light Scattering Properties of Pigment Suspensions", *J. Opt. Soc. Am.* 51, 975 (Sept. 1961).
- (19) Benford, Frank, "Radiation in a Diffusing Medium", *J. Opt. Soc. Am.* 36, 524 (1946).
- (20) Kubelka, Paul, "New Contributions to the Optics of Intensely Light-Scattering Materials", *J. Opt. Soc. Am.* 44, 330 (1954).
- (21) Johnson, P. D., "Absolute Optical Absorption From Diffuse Reflectance", *J. Opt. Soc. Am.* 42m 978 (Dec. 1952).
- (22) Melamed, N. T., "Optical Properties of Powders", *J. Appl. Phys.* 34, 560 (March 1963).
- (23) Simmons, E. L., "An Equation Relating the Diffuse Reflectance of Weakly Absorbing Powdered Samples to the Fundamental Optical Parameters", *Optica Acta* 18, 59-68 (1971).
- (24) Johnson, P. D., "Optical Absorption and Diffuse Reflectance of Powders", *J. Appl. Phys.* 35, 334 (Feb. 1964).
- (25) Dunn, S. T., "Flux Averaging Devices for the Infrared", *N. B. S. Tech. Note*, 279 (1965).
- (26) Derksen, W. L. and T. I. Monahan, "A Reflectometer for Measuring Diffuse Reflectance in the Visible and Infrared Regions", *J. Opt. Soc. Am.* 42, 263 (April 1952).
- (27) Shibata, K., "Simple Absolute Method for Measuring Diffuse Reflectance Spectra", *J. Opt. Soc. Am.* 47, 172 (February 1957).
- (28) Jacquez, J. A. and H. F. Kuppenheim, "Theory of the Integrating Sphere", *J. Opt. Soc. Am.* 45, 460 (June 1955).
- (29) Hardy, A. C. and O. W. Pineo, "The Errors Due to the Finite Size of

- Holes and Sample in Integrating Spheres", J. Opt. Soc. Am. 21, 502 (Aug. 1931).
- (30) Olson, O. H. and D. A. Pontarelli, "Asymmetry of an Integrating Sphere", App. Opt. 2, 631 (June 1963).
- (31) Smith, W. J., "Optical Materials and Coatings", Modern Optical Engineering, McGraw-Hill Book Co., New York, 1966, p. 176.
- (32) Beattie, W. H. and W. S. Gallaway, "Light-Scattering Accessory for Beckman DK Spectrophotometers", Appl. Opt. 4, 1607 (Dec 1965).
- (33) Operating and Maintenance Instructions for Model DK-1 Spectrophotometer, 355-B, Beckman Instruments, Inc., Fullerton, California, 1955.
- (34) Budde, W., "Standards of Reflectance", J. Opt. Soc. Am. 50, 217 (1960).
- (35) Middleton, W. E. K. and C. L. Sanders, "An Improved Sphere Paint", Illuminating Engineering 48, 254 (May 1953).
- (36) Rosa, E. B. and A. H. Taylor, "Theory, Construction, and Use of the Photometric Integrating Sphere", Sci. Papers Natl'. Bur. Sd. (U.S.) 447 (1922).
- (37) Brandenberg, W. M. and J. T. Neu, "Reflectance of Imperfect Diffusers", J. Opt. Soc. Am. 56, 100 (January 1966).
- (38) Middleton, W. E. K. and C. L. Sanders, "The Absolute Spectral Diffuse Reflectance of Magnesium Oxide", J. Opt. Soc. Am. 41, 422 (June 1951).
- (39) Middleton, W. E. K. and C. L. Sanders, "The Absolute Spectral Diffuse Reflectance of Magnesium Oxide in the Near Infrared", J. Opt. Soc. Am. 43, 58 (January 1953).
- (40) "Preparation of a Magnesium Oxide Standard for Spectral Reflectivity", American Society for Testing Materials, Designation D 986-50.
- (41) McAloren, J. T., "A Reproducible Magnesium Oxide Standard for Reflectance Measurement From 0.3 to 2.6 Microns", Nature 195, 797 (Aug. 1962).
- (42) Rutledge, J. L., "Surface Parameters of Stannic Oxide in Powder, Ceramic, and Gel Form by Nitrogen Absorption Techniques", Proc. Okla. Acad. Sci. 46, 137-141 (1966).
- (43) Matthews, H. E., "Photoconductivity and Surface Effects in Zn Doped Polycrystalline Stannic Oxide", Interim Report SS-3 NASA Grant Ns G609 (1967).
- (44) Matthews, H. E., "A Preliminary Study of Certain Electrical Proper-

ties of Stannic Oxide Ceramics", M.S. Thesis (May 1965).

- (45) Schatz, Elihu A., "Reflectance Variables of Compacted Powders", Proceedings of A.C.S. Symposium on Reflectance Spectroscopy (1967).
- (46) Schatz, Elihu A., "Effect of Pressure on the Reflectance of Compacted Powders", J. Opt. Soc. Am. 56, 389 (March 1966).
- (47) Harrick, N. J., "Total Internal Reflection and its Application to Surface Studies", Ann. N.Y. Acad. Sci. 101, 928 (1963).
- (48) Schatz, Elihu A., "Spectral Reflectance of Sintered Oxides", J. Am. Ceram. Soc. 51, 287 (1967).
- (49) Moss, T. S., "Dispersion Theory", Optical Properties of Semiconductors, Academic Press, (1959), pp. 15-29, 38-43.
- (50) Fochs, F. D., "The Measurement of the Energy Gap of Semiconductors From Their Diffuse Reflection Spectra", Proc. Phys. Soc. London 69, 70-75 (January 1956).
- (51) McLean, T. P., "The Absorption Edge Spectrum of Semiconductors", Progr. in Semiconductors 5, 59 (1960).
- (52) Karvaly, B. and I. Hevesi, "Investigation on Diffuse Reflectance Spectra of V_2O_5 Powder", Z. Naturforsch 26a, 245 (1971).
- (53) Smith, R. A., Semiconductors, Cambridge, Mass., Cambridge University Press, 1959, p. 189.
- (54) Filimonov, "Changes in the Infrared Absorption of Certain Semiconducting Absorbants Under Ultraviolet Illumination", Optika i Spektrosk 8, 270-272, (February 1960).
- (55) "Solar-Radiation Induced Damage to Optical Properties of ZnO-Type Pigments", Locheed Palo Alto Research Lab Report, June 1967.

VITA^y

Lee Roy Matthiesen

Candidate for the Degree of

Doctor of Education

Thesis: SPECTRAL REFLECTANCE OF POLYCRYSTALLINE STANNIC OXIDE

Major Field: Higher Education

Biographical:

Personal Data: Born in Ardmore, Oklahoma, June 14, 1939, the son of Paul and Cecil Matthiesen.

Education: Graduated from Enid High School in Enid, Oklahoma, in 1956; received a Bachelor of Science degree from Oklahoma State University with a major in Education in 1960; received a Master of Science degree from Kansas State Teachers College, Emporia, Kansas, with a major in Physical Science in 1964; received a Doctor of Education degree from Oklahoma State University, July, 1972.